



CHORUS

This is the accepted manuscript made available via CHORUS. The article has been published as:

Generic Mechanism of Optimal Energy Transfer Efficiency: A Scaling Theory of the Mean First-Passage Time in Exciton Systems

Jianlan Wu, Robert J. Silbey, and Jianshu Cao

Phys. Rev. Lett. **110**, 200402 — Published 13 May 2013

DOI: [10.1103/PhysRevLett.110.200402](https://doi.org/10.1103/PhysRevLett.110.200402)

Generic Mechanism of Optimal Energy Transfer Efficiency: A Scaling Theory of the Mean First Passage Time in Exciton Systems

Jianlan Wu,^{1,2} Robert J. Silbey*,¹ and Jianshu Cao^{†1}

¹*Department of Chemistry, MIT, 77 Massachusetts Ave, Cambridge, MA, 02139, USA*

²*Physics Department, Zhejiang University,
38 ZheDa Road, Hangzhou, Zhejiang, 310027, China*

(Dated: April 15, 2013)

Abstract

An asymptotic scaling theory is presented using the conceptual basis of trapping-free subspace (i.e., orthogonal subspace) to establish the generic mechanism of optimal efficiency of excitation energy transfer (EET) in light-harvesting systems. A quantum state orthogonal to the trap will exhibit noise-assisted transfer, clarifying the significance of initial preparation. For such an initial state, the efficiency is enhanced in the weak damping limit ($\langle t \rangle \sim 1/\Gamma$), and suppressed in the strong damping limit ($\langle t \rangle \sim \Gamma$), analogous to Kramers' turnover in classical rate theory. An interpolating expression, $\langle t \rangle = A/\Gamma + B + C\Gamma$, quantitatively describes the trapping time over the entire range of the dissipation strength, and predicts the optimal efficiency at $\Gamma_{\text{opt}} \sim J$. In the presence of static disorder, the scaling law of transfer time with respect to dephasing rate changes from linear to square root, suggesting a weaker dependence on the environment. The prediction of the scaling theory is verified in a symmetric dendrimer system by numerically exact quantum calculations. Though formulated in the context of EET, the analysis and conclusions apply in general to open quantum processes, including electron transfer, fluorescence emission, and heat conduction.

* Dedicated to the memory of Prof. Robert J. Silbey

[†] Electronic address: jianshu@mit.edu

The optimization of the excitation energy transfer (EET) process presents a challenge for understanding photosynthetic systems as well as for designing efficient solar energy devices. Multi-dimensional spectra have allowed detailed probes of EET dynamics, revealing signatures of quantum coherence [1–4]. In contrast to the common belief that noise retards motion and coherence enhances mobility, the EET efficiency reaches the maximum at an intermediate level of noise, leading to the notion of noise-enhanced energy transfer [5–10]. Fermi’s golden rule rate provides a simple interpretation and suggests that stochastic resonance between the donor and acceptor enhances EET efficiency [8–10]. Another possible mechanism is that noise suppresses destructive interference between pathways [8, 9]. The situation is further complicated by the findings that initial preparation, coherence of incident photons, site energy, spatial correlation, static disorder, and various approximations invoked in quantum master equations can all play a role in establishing optimal efficiency [10–15]. Therefore, a general mechanism for optimization in an arbitrary EET system accompanying all these effects is clearly needed but has not yet been formulated. In this Letter, we utilize the concept of trapping-free subspace (i.e., orthogonal subspace) to bring together all of the above considerations into a unified framework, that allows us to establish asymptotic scaling relations under both dynamic and static disorder and construct the generic functional form of optimal EET efficiency.

Model. — We consider a light-harvesting EET system (see examples in Fig. 1) described by the quantum equation of motion for the reduced density matrix of the single excitation manifold [9], $\dot{\rho}(t) = -\mathcal{L}\rho(t)$. Here, the Liouville superoperator $\mathcal{L} = \mathcal{L}_{\text{sys}} + \mathcal{L}_{\text{dissip}} + \mathcal{L}_{\text{trap}} + \mathcal{L}_{\text{decay}}$ comprises four terms, each describing a distinct dynamic process: (i) $\mathcal{L}_{\text{sys}}\rho(t) = (i/\hbar)[H_S, \rho(t)]$, the dynamics of the isolated system, where H_S is the system Hamiltonian; (ii) $\mathcal{L}_{\text{dissip}}$, the exciton re-distribution and dephasing within the single-excitation manifold; (iii) $\mathcal{L}_{\text{trap}}$, the trapping of excitation energy at the reaction center; (iv) $\mathcal{L}_{\text{decay}}$, the decay of the excitation energy to ground state in the form of heat or a photon. Each superoperator can be represented by a matrix defined in the Liouville space. A basic property of an EET system is its energy transfer efficiency, $q = \text{Tr} \int_0^\infty \mathcal{L}_{\text{trap}}\rho(t)dt$, where Tr denotes the trace over states. For an efficient EET system such as a light-harvesting protein complex, its nearly unit efficiency, $q \sim 1$, implies a clear time-scale separation between the decay and trapping processes. Under this condition and with a homogeneous decay rate k_d , the transfer efficiency can be approximated by $q \approx (1 + k_d\langle t \rangle)^{-1}$, where $\langle t \rangle = \text{Tr} [\mathcal{L}_0^{-1}\rho(0)]$ is the the

average trapping time for the initial density matrix $\rho(0)$, and $\mathcal{L}_0 = \mathcal{L}_{\text{sys}} + \mathcal{L}_{\text{trap}} + \mathcal{L}_{\text{dissip}}$ is the Liouville superoperator in the absence of decay [9].

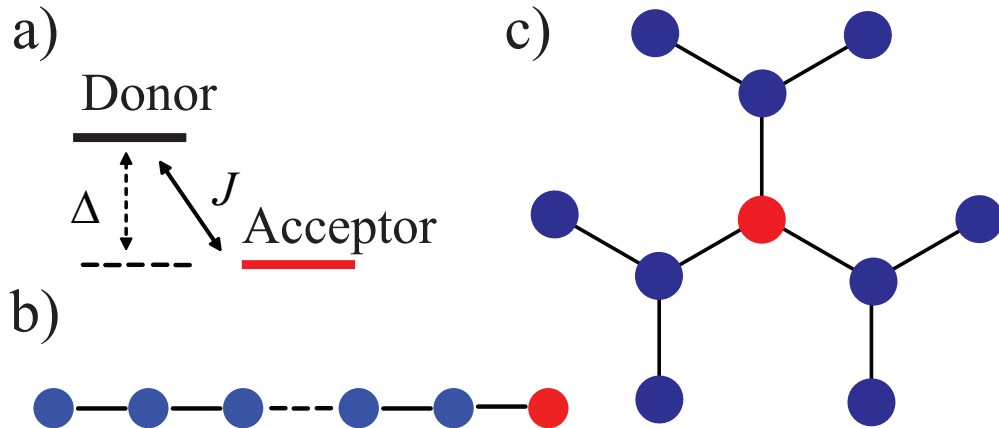


FIG. 1: Various EET systems with the trapping free subspace: a) A donor-acceptor system with a large energy mismatch ($\Delta \gg J$). b) A homogeneous N -site ($N \gg 1$) chain. c) A two-generation three-fold dendrimer [20].

The optimization of EET is simplified to the minimization of $\langle t \rangle$. For many EET systems, $\langle t \rangle$ decreases with increasing Γ for weak dissipation and diverges with Γ for strong dissipation, where Γ represents a characteristic dissipation strength in $\mathcal{L}_{\text{dissip}}$, e.g., the dephasing rate [5–10]. A representative curve of this dependence is plotted in Fig. 2a, where the trapping time $\langle t \rangle$ is minimal at an optimal noise level, Γ_{opt} . To understand this generic behavior, we investigate the asymptotic scaling of $\langle t \rangle$ in the strong and weak dissipation limits.

Asymptotics of the trapping time. — In the strong damping limit ($\Gamma \gg 1$), quantum coherence is quickly destroyed by noise, and energy is transferred through incoherent hops. The hopping rate k_{hop} can be estimated from Fermi’s golden rule, giving $k_{\text{hop}} \sim |J|^2/\Gamma$ for classical noise, with J the exciton coupling strength. Thus, the trapping time diverges linearly with Γ , giving

$$\langle t \rangle \sim k_{\text{hop}}^{-1} \sim \Gamma/|J|^2. \quad (1)$$

For a quantum bath, the Γ -dependence of k_{hop} becomes more complicated, exhibiting thermal activation, but can follow the linear Γ function in Eq. (1) for relatively large values of damping, as verified by the computational results of the hierarchy equation for a dendrimer system in this Letter.

In the opposite limit of weak damping ($\Gamma \rightarrow 0$), energy transfer can be enhanced by dynamic noise such that $\langle t \rangle$ decreases with increasing Γ . Here the starting point for EET dynamics is the delocalized exciton basis, i.e., eigenstates of H_S . Following the secular approximation, $\langle t \rangle$ is dominated by the dynamics within the exciton population subspace, $\langle t \rangle \approx \text{Tr} \left[(\mathcal{L}_{\text{dissip};P}^E + \mathcal{L}_{\text{trap};P}^E)^{-1} \rho_P^E(0) \right]$, where the superscript E denotes the exciton representation and the subscript P denotes the population subspace. However, a set of excitons, $\Phi_{\perp} = \{|E_i\rangle\}$, orthogonal to the trapping operator, $\mathcal{L}_{\text{trap};ii}^E = 0$, are incapable of efficient energy transfer and define a trapping-free subspace Φ_{\perp} . Generally, the zero determinant for the trapping block matrix,

$$\text{Det} [\mathcal{L}_{\text{trap};P}^E] = 0, \quad (2)$$

leads to the divergence of the coherent trapping time, $\langle t \rangle|_{\Gamma=0} = \infty$. The definition of the trapping-free subspace is a generalization of the invariant subspace [8] and is closely related to the concept of decoherence-free subspace in quantum information [16]. The system-bath coupling induces interactions between the trapping-free and other exciton states, resulting in population depletion from Φ_{\perp} . Thus, dissipation of Φ_{\perp} dominates the average trapping time. For nonzero population in Φ_{\perp} , the leading order of $\langle t \rangle$ is given by the survival time in the orthogonal exciton subspace,

$$\langle t \rangle \approx \sum_{i \in \Phi_{\perp}} (L_{\text{dissip};ii}^E)^{-1} \rho_i^E(0) / \Gamma, \quad (3)$$

where $L_{\text{dissip}}^E = \mathcal{L}_{\text{dissip}}^E / \Gamma$ is the rescaled Liouville superoperator in the exciton representation, independent of Γ for $\Gamma \rightarrow 0$. In many EET systems, the orthogonal condition in Eq. (2) may not be rigorously satisfied, then $\langle t \rangle$ does not completely diverge in the coherent limit. In general, the trapping time for weak dissipation can be expanded as

$$\langle t \rangle \sim c_0 + c_1 / (\Gamma + \Gamma_1) + c_2 / (\Gamma + \Gamma_2) + \dots, \quad (4)$$

where $\{\Gamma_1, \Gamma_2, \dots\}$ is independent of the initial condition, but $\{c_0, c_1, c_2, \dots\}$ depends on the initial condition. Equation (4) recovers the asymptotic $1/\Gamma$ -scaling in Eq. (3) under the condition of $\Gamma_{k(\geq 1)} \rightarrow 0$.

Generality. — The two scaling relations in the asymptotic regimes are based on general physical arguments and independent of specific details such as the system-bath coupling,

bath spectral density, truncation method, and approximations in the quantum master equation. Combining Equations (1) and (3), we can show that the optimal condition,

$$\Gamma_{\text{opt}} \sim \left\{ \sum_{i \in \Phi_{\perp}} (L_{\text{dissip};ii}^E)^{-1} \rho_i^E(0) \right\}^{1/2} |J| \propto |J|, \quad (5)$$

depends on the system Hamiltonian as well as the initial condition. The general Γ -dependence follows the interpolating functional form,

$$\langle t \rangle = A/\Gamma + B + C\Gamma, \quad (6)$$

where A , B , C are fitting coefficients. In fact, the optimal efficiency is analogous to the Kramers turnover in reaction rate theory, where the two scaling regimes correspond to energy diffusion and spatial diffusion, respectively [17, 18]. The change of the reaction coordinate from energy to spatial position in classical rate theory corresponds to the change of basis set from excitons to local sites in energy transfer theory. However, the analogy to classical rate theory is limited to the orthogonal subspace and does not apply to the non-orthogonal subspace, where coherent energy transfer does not display a turnover.

The trapping-free subspace defined in Eqs. (2) can be realized in various systems. (i) In an inhomogeneous system with large energy mismatches (see Fig. 1a), the orthogonality can arise from a vanishingly small overlap between the donor and acceptor. This situation can be well described by Fermi's golden rule and qualitatively explains the optimal efficiency in FMO [10, 19]. (ii) In a spatially extended system, the orthogonality can arise because the overlap coefficient of a local site with the trap decreases with the system size, e.g., a long, homogeneous chain system (see Fig. 1b). (iii) In a system with intrinsic symmetry, a subset of excitons are incompatible with the symmetry of $\mathcal{L}_{\text{trap}}$, thus leading to orthogonality. The fully-connected network [8] and the dendrimer in Fig. 1c are examples of such topological symmetry. The orthogonality due to symmetry in case (iii) is rigorous, whereas the orthogonality in cases (i) and (ii) is approximate. In cases (i) and (ii), $\langle t \rangle$ does not diverge at $\Gamma = 0$ but can still lead to an optimal efficiency because of approximate orthogonality. On the other hand, if the initial state is specially prepared to be orthogonal to the trapping-free subspace, i.e., $\rho_{\perp} = 0$ in Eq. (3) or $c_{k(\geq 1)} = 0$ in Eq. (4), the $1/\Gamma$ -scaling disappears and $\langle t \rangle$ is almost a constant minimum in the weak damping limit. Such a change in the Γ -dependence of $\langle t \rangle$ is observed in the N -site homogeneous chain as the initial state moves along the chain.

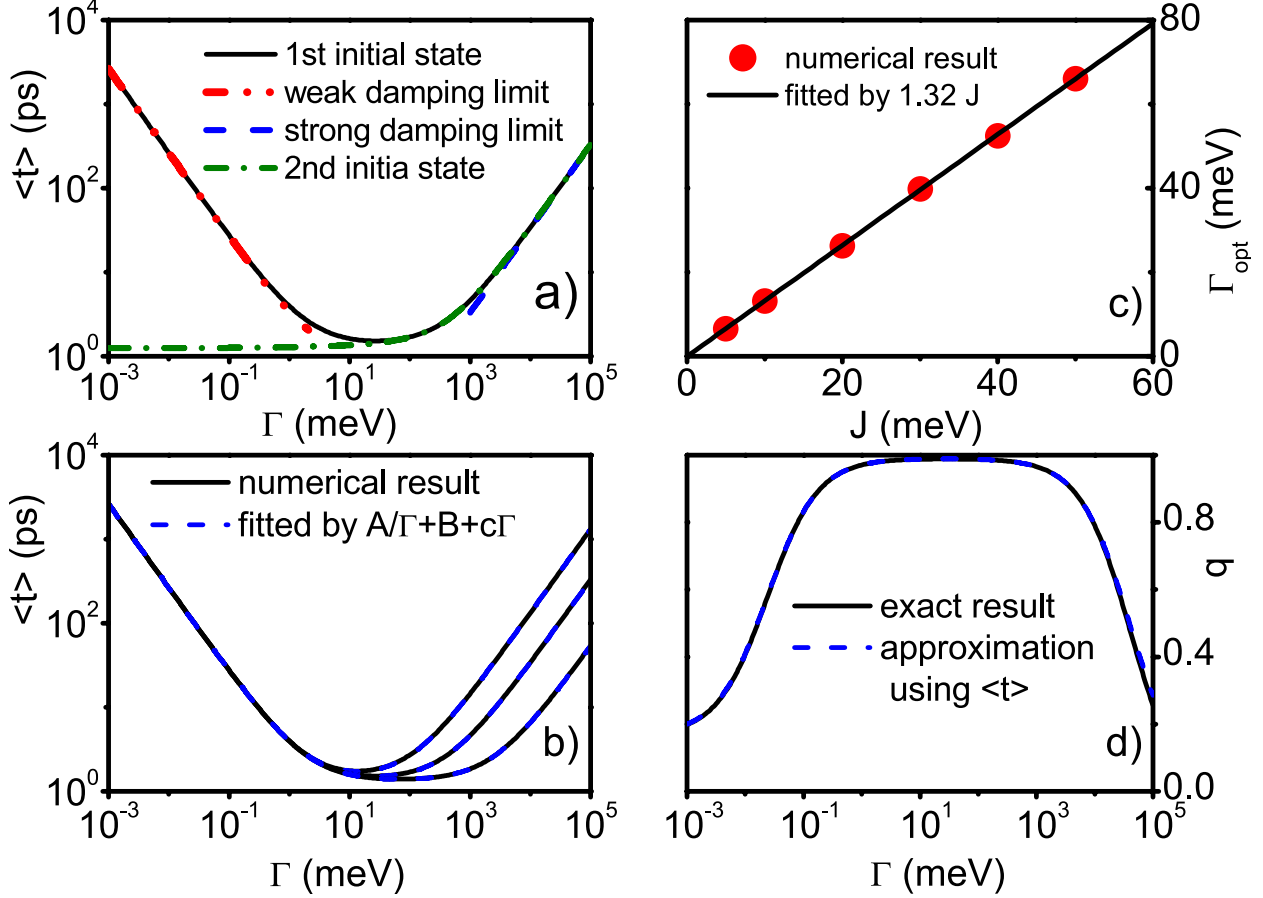


FIG. 2: EET of the dendrimer (Fig. 1c) using the HSR model. a) The trapping time $\langle t \rangle$ vs. the pure dephasing rate Γ . For the first initial condition with $\rho_{\perp} \neq 0$ (see text), the solid, dashed, and dashed-dotted-dotted lines are the full calculation, from Eq. (1), and from Eq. (3), respectively. The dashed-dotted line is the result for the second initial condition with $\rho_{\perp} = 0$ (see text). b) The functional form in Eq. (6) (dashed lines) quantitatively fits numerical results of $\langle t \rangle$ (solid lines) for different site-site couplings, $J=10, 20, 50$ meV (from top to bottom). c) The optimal Γ is a linear function of the site-site coupling J . d) The transfer efficiency q vs. Γ for the first initial condition. The dashed line is the exact result while the solid line is from the approximation using $\langle t \rangle$ [23].

An example — To verify the above analysis, we investigate a two-generation three-fold dendrimer depicted in Fig. 1c [20]. A tight-binding model is used for the system Hamiltonian, giving $H_{S;ij} = \varepsilon_i \delta_{ij} |i\rangle\langle i| + J_{ij} (1 - \delta_{ij}) |i\rangle\langle j|$, where $|i\rangle$ represents a localized state at site i . All the site energies ε_i are identical and the site-site interaction $J_{ij} = 20$ meV are constant for all pairs of connected sites. The center site is the trap site with rate $k_t = 5$ meV. The decay process is characterized by a homogeneous rate $k_d = 5$ μ eV. We approximate

dissipation by the Haken-Strobl-Reineker (HSR) model [21, 22] and consider homogeneous pure dephasing, $\mathcal{L}_{\text{dissip};ij} = (1 - \delta_{i,j})\Gamma$, where Γ is the pure dephasing rate. The orthogonal subspace of this dendrimer system consists of seven exciton states. We compare two different cases of initial preparation. In the first case, an incoherent population is evenly distributed at six outer sites with $\rho_{\perp}(0) \neq 0$. The trapping time is plotted as a function of Γ in Fig. 2a. The divergence of $\langle t \rangle$ in the strong and weak dephasing limits agrees excellently with the asymptotic behaviors predicted in Eqs. (1) and (3), respectively. Furthermore, Eq. (6) can quantitatively describe the cross-over and fit the trapping time for the complete range of Γ . The resulting Γ_{opt} in Fig. 2c is proportional to J , in agreement with Eq. (5). Figure 2d shows that our approximate equation using $\langle t \rangle$ provides a quantitatively accurate description for the EET efficiency [23]. In the second case, a coherent state is evenly distributed at the six outer sites with $\rho_{\perp}(0) = 0$. The trapping time does not diverge since no initial population exists in Φ_{\perp} . Above a threshold at the intermediate dephasing rate, $\langle t \rangle$ changes from a plateau to the same linearly increasing function of Γ . This calculation confirms that dynamic noise can enhance the EET only if components of the initial state are orthogonal to the trapping process.

Static disorder. — We introduce an energy disorder $\delta\varepsilon_i$ at each site i , that follows the Gaussian distribution, $P(\delta\varepsilon_i) = \exp[-(\delta\varepsilon_i^2/(2\sigma_i^2))]/\sqrt{2\pi}\sigma_i$, where σ_i is the variance of disorder. The resulting ensemble average is given by $\langle x \rangle_{\sigma} = \Pi_i \int x(\delta\varepsilon_i)P(\delta\varepsilon_i)d\delta\varepsilon_i$ with $x = \langle t \rangle$ or q . With the first initial condition, we present the results of $\langle \langle t \rangle \rangle_{\sigma}$ and $\langle q \rangle_{\sigma}$ obtained from a Monte Carlo simulation of 10^5 samples. As shown in Fig. 3a, static disorder is irrelevant in the strong dephasing limit ($\Gamma \gg \sigma$). In the weak dephasing limit ($\Gamma \ll \sigma \ll J$), static disorder can destroy the orthogonality in Eq. (2) and induce a large reduction of the trapping time. However, if the random energy disorder falls below σ' ($\sim \sqrt{\Gamma}$), the weak orthogonality is preserved and $\langle t \rangle$ diverges. The new asymptotic relation in the weak dephasing limit is given by an integral over these small disorders,

$$\langle \langle t \rangle \rangle_{\sigma} \sim \int_{-\sigma'}^{\sigma'} d\delta\varepsilon P(\delta\varepsilon) \langle t \rangle|_{|\delta\varepsilon| < \sigma'} \sim \frac{c}{\sigma\sqrt{\Gamma}}, \quad (7)$$

where $\delta\varepsilon$ describes the effective in-phase energy fluctuation over all the sites, $P(\delta\varepsilon) \sim 1/\sigma$ is the probability distribution, and $\langle t \rangle|_{|\delta\varepsilon| < \sigma'} \approx \langle t \rangle|_{\delta\varepsilon=0} \sim 1/\Gamma$ is approximately uniform within this regime. The pre-factor c depends on $\rho(0)$, H_S and k_t . To confirm the asymptotic relation in Eq. (7), we calculate the weak-dephasing $\langle \langle t \rangle \rangle_{\sigma}$ as a function of σ for different

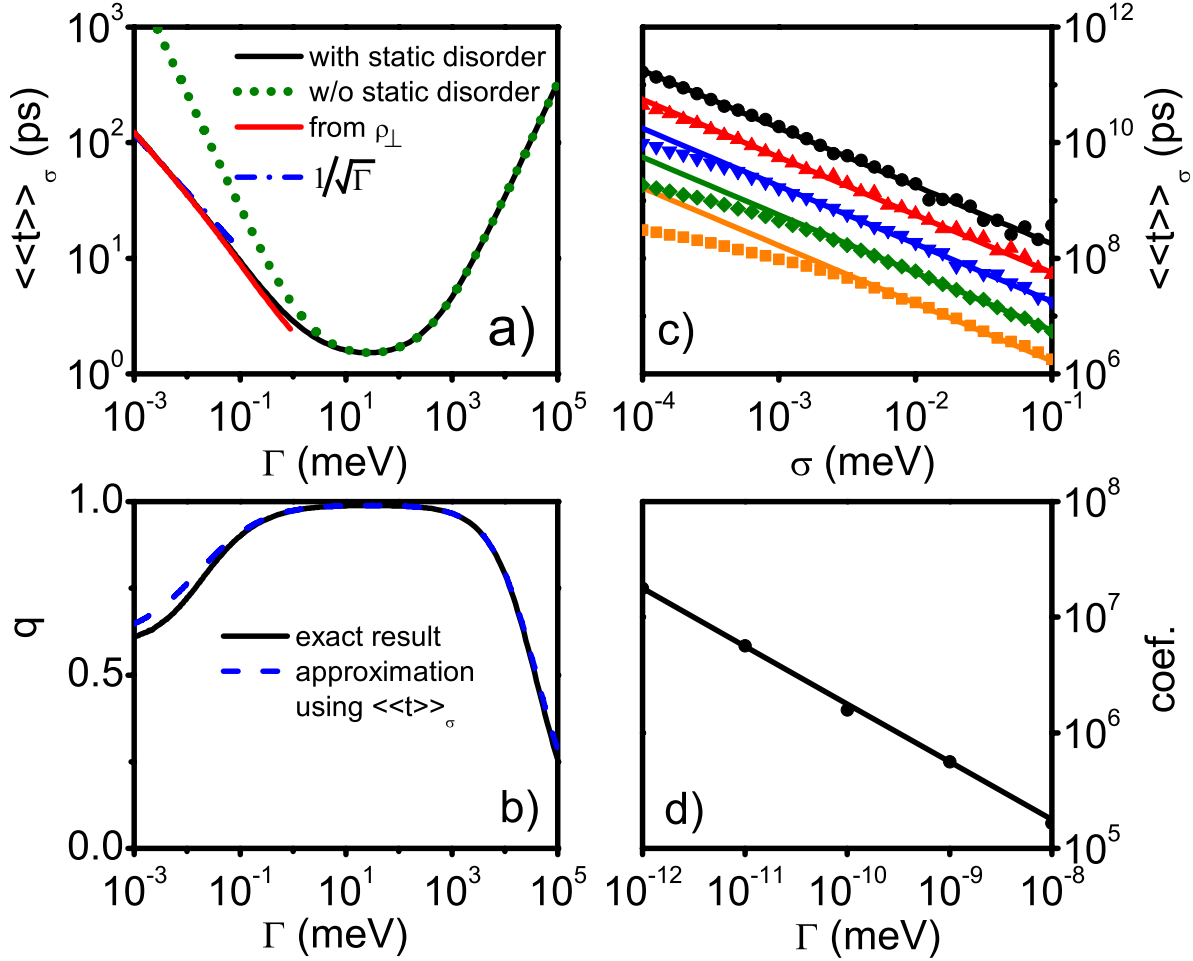


FIG. 3: a)-b) The ensemble-averaged EET of the dendrimer (Fig. 1c) in the HSR model with a static disorder $\sigma = 4$ meV. a) The solid line is the simulation result of $\langle\langle t \rangle\rangle_\sigma$, referenced by the dotted line without σ from Fig. 2a. The dashed line is from Φ_\perp , and the dashed-dotted line is the fitting result of $1/\sqrt{\Gamma}$. b) $\langle q \rangle_\sigma$ vs. Γ : the solid line is the ensemble average from the original definition whereas the dashed line is from the approximation using $\langle\langle t \rangle\rangle_\sigma$ [23]. c) The weak-dephasing σ -dependence of $\langle\langle t \rangle\rangle_\sigma$, with $\Gamma = 10^{-12}, 10^{-11}, 10^{-10}, 10^{-9}, 10^{-8}$ meV (from top to bottom). Symbols denote simulation results, whereas the solid lines are fitted with $\langle\langle t \rangle\rangle_\sigma = c'/\sigma$. d) The fitting coefficient c' (circles) can be further fitted by $c' = c/\sqrt{\Gamma}$ (the solid line).

values of Γ and rigorously establish the scaling relation predicted in Figs. 3c-d. Interestingly, as shown in Fig. 3b, the zero dephasing efficiency $\langle q |_{\Gamma=0} \rangle_\sigma$ is drastically enhanced from 0.2 to 0.8 with disorder $\sigma = J/5$. Our calculations suggest that nature can use both static and dynamic disorders cooperatively to achieve efficient and robust energy transfer.

The Quantum Drude-Lorentz Bath. — In above calculation, the dissipation is modeled

by the classical white noise, i.e., the HSR model. To further verify the predictions of our scaling theory, we consider a quantum bath described by the Drude-Lorentz spectral density, $J(\omega) = (2\hbar/\pi)\lambda\omega\omega_D/(\omega^2 + \omega_D^2)$, where λ is the reorganization energy and ω_D is the Debye frequency ($\omega_D^{-1} = 50$ fs). The room temperature $T = 300$ K is applied with the high- T approximation, $\coth(\beta\omega/2) \approx 2/\beta\omega$. The quantum dissipative dynamics of the Drude-Lorentz bath can be reliably calculated using the hierarchy equation of motion [24, 25]. In Fig. 4, $\langle t \rangle$ is plotted as a function of λ , which represents the dissipation strength. The results of the Drude-Lorentz bath follow our scaling theory and agree qualitatively with the results of the HSR model in Figs. 2 and 3. For weak dissipation ($\lambda \ll 1$ meV), the trapping time under the first initial condition ($\rho_{\perp} \neq 0$) follows $1/\lambda$ scaling as predicted by Eq. (3), and the λ -dependence changes to $1/\sqrt{\lambda}$ with the static disorder ($\sigma = 1$ meV) as predicted by Eq. (7). Under the second initial state ($\rho_{\perp} = 0$), the noise-enhanced energy transfer disappears and $\langle t \rangle$ weakly increases for $\lambda < 0.1$ meV. For strong dissipation ($\lambda > 1$ meV), all three $\langle t \rangle$ - λ dependencies collapse into a single curve, indicating that classical hopping kinetics is nearly independent of initial quantum coherence and static disorder. After replacing Γ with λ , Eq. (6) can also quantitatively describe $\langle t \rangle$ over a broad range of λ , i.e., the linear λ -scaling predicted by Eq. (1) is reliable in the intermediately strong damping regime ($1 \text{ meV} < \lambda < 40 \text{ meV}$). With the change of the site-site coupling J , this functional form remains applicable (see Fig. 4b), but the J -dependencies of the coefficients A and C in Eq. (6) becomes more complicated than those in the HSR model. Consequently, the optimal λ weakly deviates from the linear function of J but still numerically follows $\lambda_{\text{opt}}/\text{meV} \sim (J/\text{meV})^{1.41}$ for $J \leq 75$ meV (see Fig. 4c). In the activation regime ($\lambda > 40$ meV), $\langle t \rangle$ gradually becomes an exponential function of λ due to the presence of energy barrier. Therefore, our scaling theory is applicable to a non-Markovian quantum bath.

Conclusion. — In this Letter, we demonstrate that the generic mechanism of noise enhanced EET is to assist energy flow out of the orthogonal exciton subspace, and the competition between noise-enhanced EET in the weak dissipation regime and noise-induced suppression in the strong dissipation regime leads to an optimal efficiency. We determine the scaling relations of the average trapping time in these two regimes and use the asymptotic relations to interpolate the efficiency over the entire parameter space and qualitatively predict the optimal noise. The presence of static disorder reduces the exponent of divergence in the weak-dissipation limit and thus makes the EET process more robust against noise.

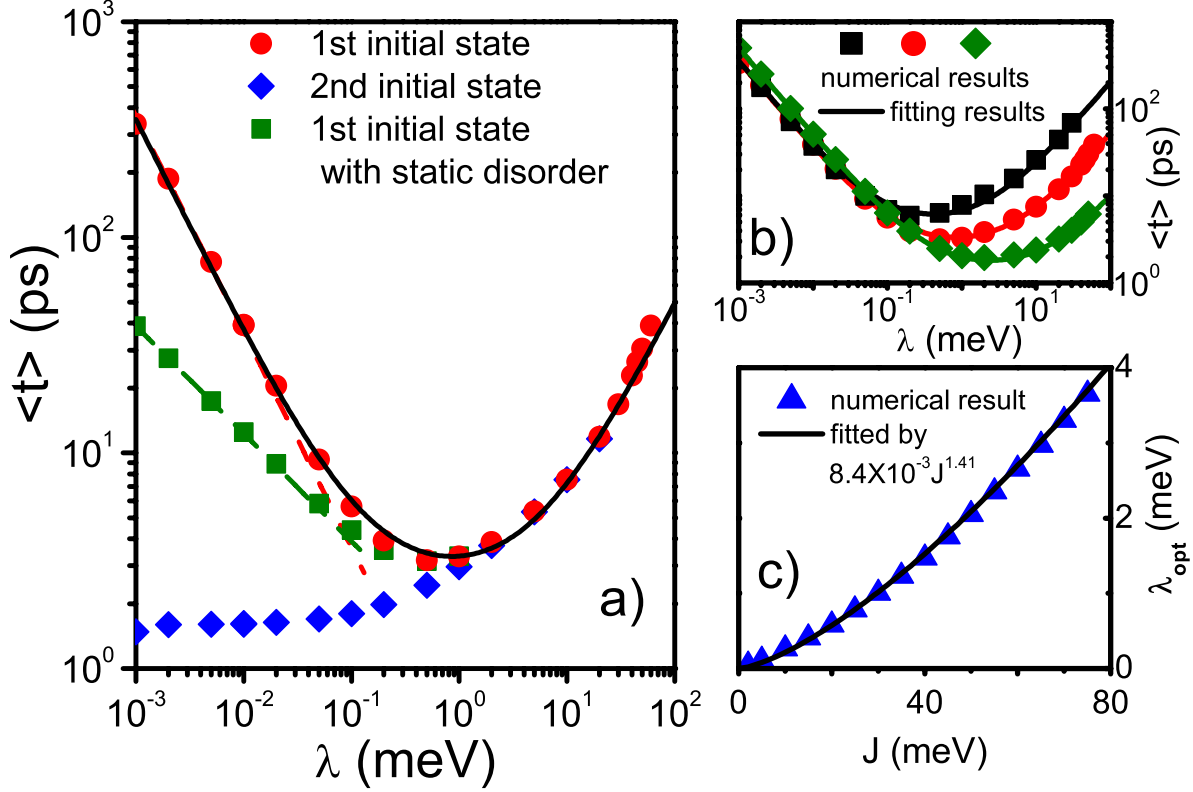


FIG. 4: a) The trapping time $\langle t \rangle$ vs. the reorganization energy λ calculated by the hierarchy equation, for the dendrimer (Fig. 1c) with $J = 20$ meV and a Drude-Lorentz bath. The circles are from the first initial condition; the diamonds are from the second initial condition; the squares are from the first initial condition with a static disorder $\sigma = 1$ meV. The $1/\lambda$ - and $1/\sqrt{\lambda}$ -scalings are shown for the circles and squares, respectively. The solid line from Eq. (6) fits the numerical result (circles). b) Equation (6) is used to fit $\langle t \rangle$ for $J=10, 20, 50$ meV (from top to bottom). c) The optimal λ approximately follows $\lambda_{\text{opt}}/\text{meV} = 8.4 \times 10^{-3}(J/\text{meV})^{1.41}$ for $J \leq 75$ meV.

Using the HSR model and the quantum Drude-Lorentz bath, we verify the predictions of the scaling theory in an example dendrimer system. Especially, the numerically accurate results using the hierarchy equation demonstrate the generality of our scaling theory. Our analysis is not limited to EET but also applies in general to electron transfer, fluorescence emission, heat conduction and other open quantum processes.

This work was supported by grants from the National Science Foundation (CHE-1112825) and DARPA (N66001-10-1-4063). JC is partially supported by the Center for Excitonics funded by the US Department of Energy (DE-SC0001088). JW acknowledges partial support from the Fundamental Research Funds for the Central Universities in China (2011QNA3005)

and the National Science Foundation of China (21173185).

- [1] G. S. Engel, et. al., Nature **446**, 782 (2007).
- [2] H. Lee, Y. C. Cheng, and G. R. Fleming, Science **316**, 1462 (2007).
- [3] E. Collini, et. al., Nature **463**, 644 (2010).
- [4] G. Panitchayangkoon, et. al. PNAS **107**, 12766 (2010)
- [5] K. Gaab and C. Bardeen, J. Chem. Phys. **121**, 7813 (2004).
- [6] S. M. Vlaming, V. A. Malyshev, and J. Knoester, J. Chem. Phys. **127**, 154719 (2007)
- [7] P. Rebentrost, et. al., New J. Phys. **11**, 033003 (2009).
- [8] F. Caruso, et. al., J. Chem. Phys. **131**, 105106 (2009).
- [9] J. S. Cao and R. J. Silbey, J. Phys. Chem. A **113**, 13825 (2009).
- [10] J. L. Wu, F. Liu, Y. Shen, J. S. Cao, and R. J. Silbey, New J. Phys. **12**, 105012 (2010).
- [11] M. Sarovar, A. Ishizaki, G. R. Fleming, and K. B. Whaley Nature Phys. **6**, 462 (2010).
- [12] J. Moix, J. L. Wu, P. F. Huo, D. F. Coker, and J. S. Cao, J. Phys. Chem. Lett. **2**, 3045 (2011).
- [13] M. Mohseni, A. Shabani, S. Lloyd, and H. Rabitz, arXiv:1104.4812 (2011).
- [14] P. Brumer and M. Shapiro, PNAS **109**, 19575 (2012).
- [15] T. Mancal and L. Valkunas, New J. Phys. **12** 065044 (2010).
- [16] D. A. Lidar, I. L. Chuang and K. B. Whaley, Phys. Rev. Lett. **81**, 2594 (1998).
- [17] J. E. Straub, M. Borkovec, and B. J. Berne, J. Chem. Phys. **84**, 1788 (1986).
- [18] E. Pollak, H. Grabert, and P. Hänggi, J. Chem. Phys. **91**, 4073 (1989).
- [19] J. L. Wu, F. Liu, J. Ma, R. J. Silbey, and J. S. Cao, J. Chem. Phys. **137**, 174111 (2012).
- [20] C. Supritz, A. Engelmann, and P. Reineker, J. Lumin. **119**, 337 (2006).
- [21] H. Haken and P. Reineker, Z. Physik **249**, 253 (1972).
- [22] H. Haken and G. Strobl Z. Phys. **262**, 35 (1973).
- [23] For small dephasing rates, $\langle t \rangle$ is replaced by $1/(\langle t \rangle^{-1} + t_0^{-1})$ in the approximation form where the constant $t_0 = (q|_{\Gamma=0}^{-1} - 1)/k_d$ corrects the zero-dissipation transfer efficiency.
- [24] Y. Tanimura and R. Kubo, J. Phys. Soc. Jpn. **58**, 101 (1989).
- [25] A. Ishizaki and G. R. Fleming, PNAS **106**, 17255 (2009).